

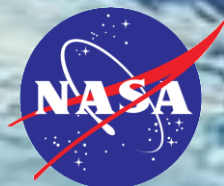
A Novel Cirrus Cloud Retrieval Method For GCM High Cloud Validations

David Mitchell
Desert Research Institute
Reno, Nevada

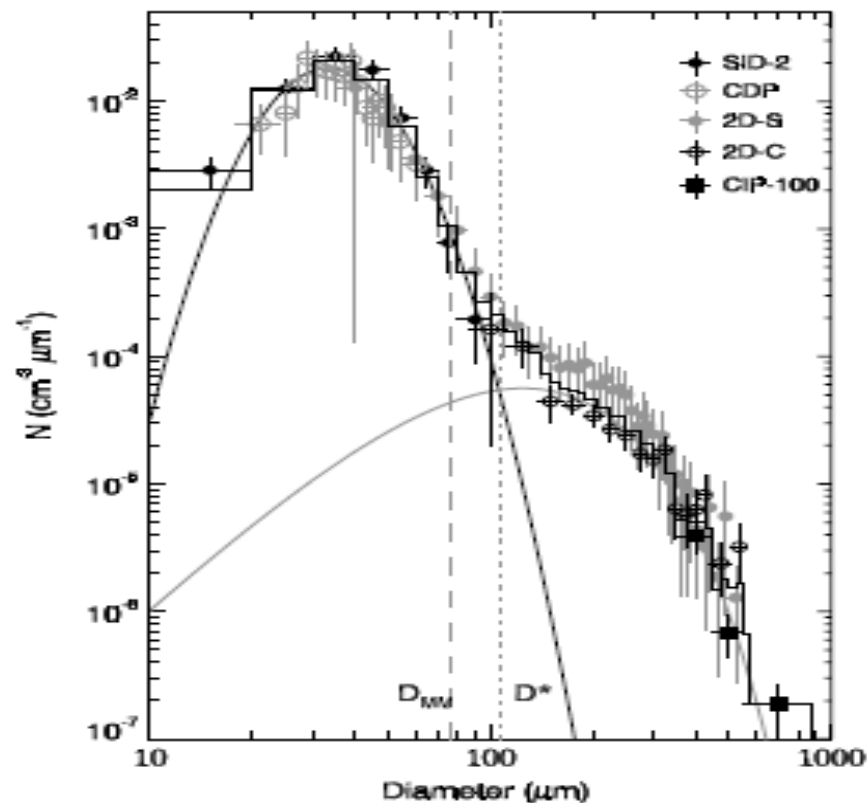
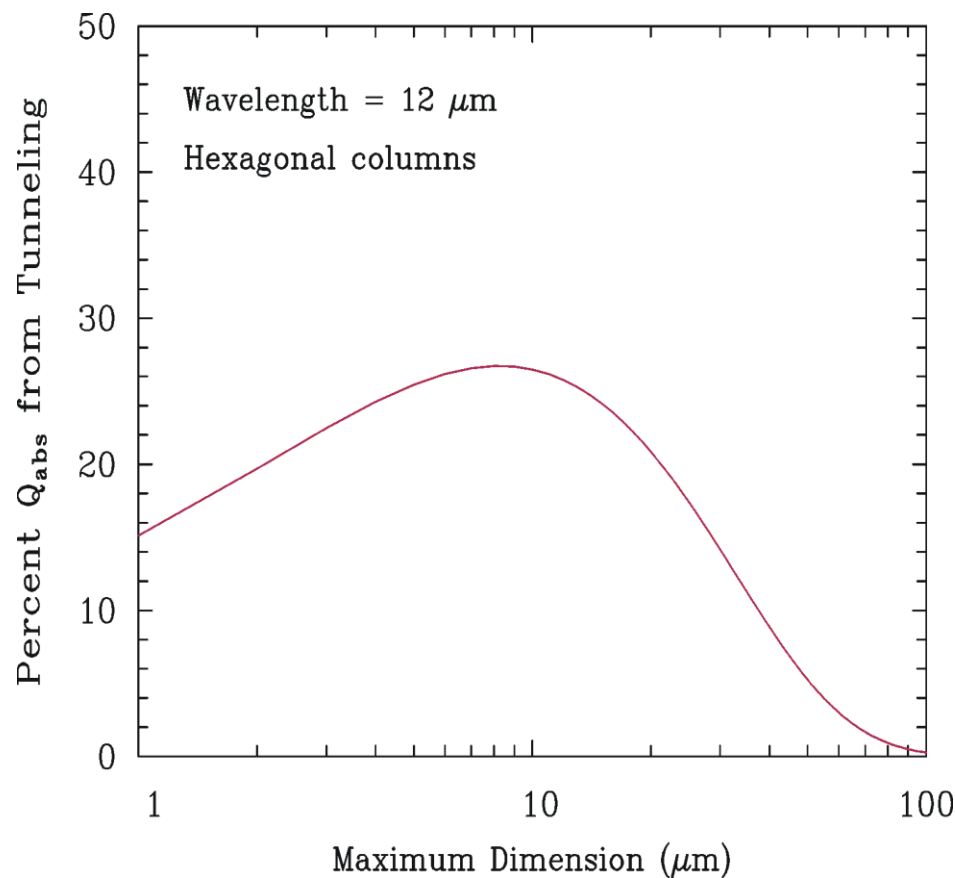
Anne Garnier
Science Systems & Applications, Inc.
Hampton, Virginia

Melody Avery
NASA Langley
Hampton, Virginia

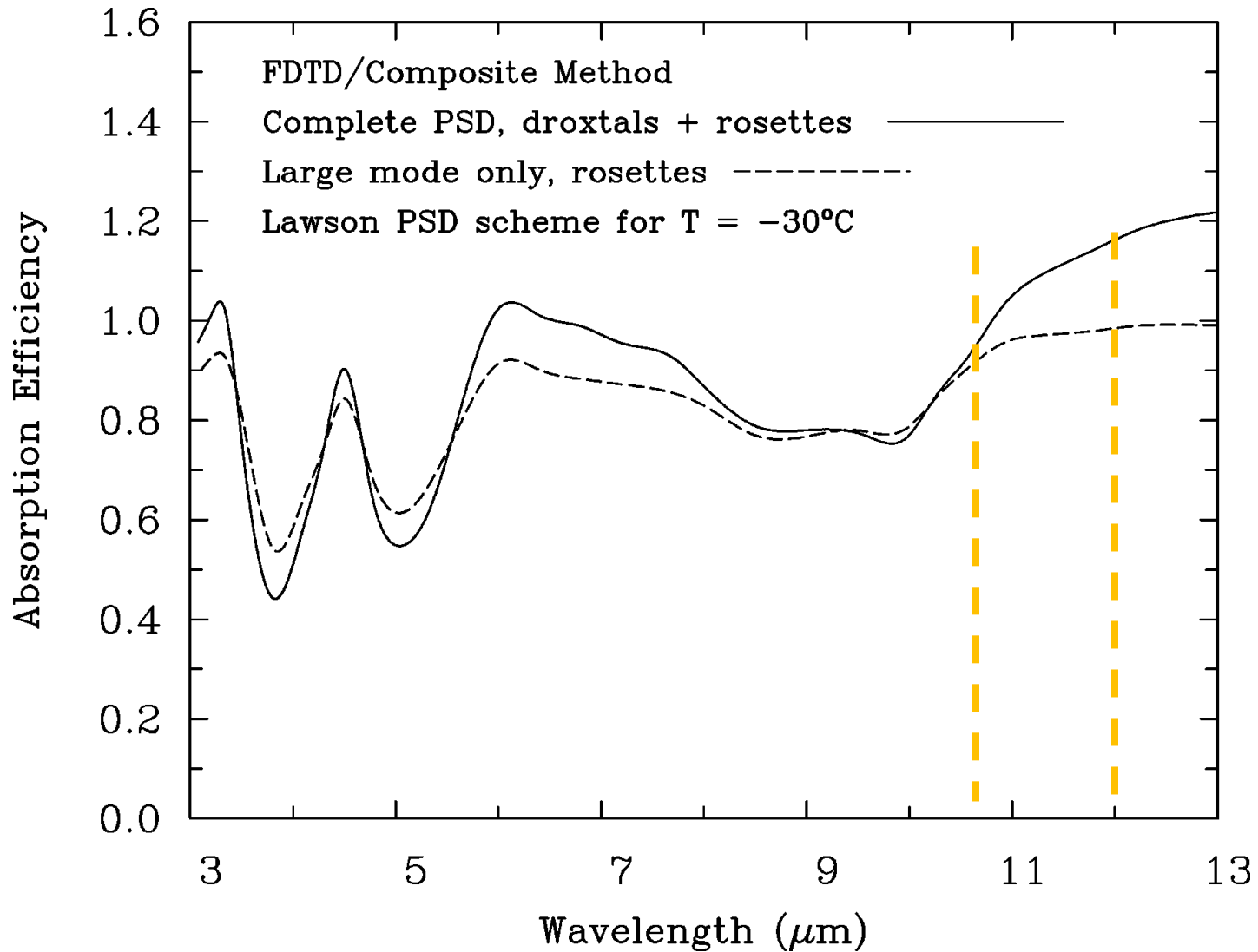
Ehsan Erfani
University of Nevada, Reno



Satellite remote sensing method: Retrieved cloud property must be sensitive to small ice crystals



$\bar{Q}_{\text{abs}}(12 \mu\text{m}) / \bar{Q}_{\text{abs}}(10.6 \mu\text{m}) =$ a measure of relative concentration of small ice crystals (Mitchell et al. 2010, JAS)



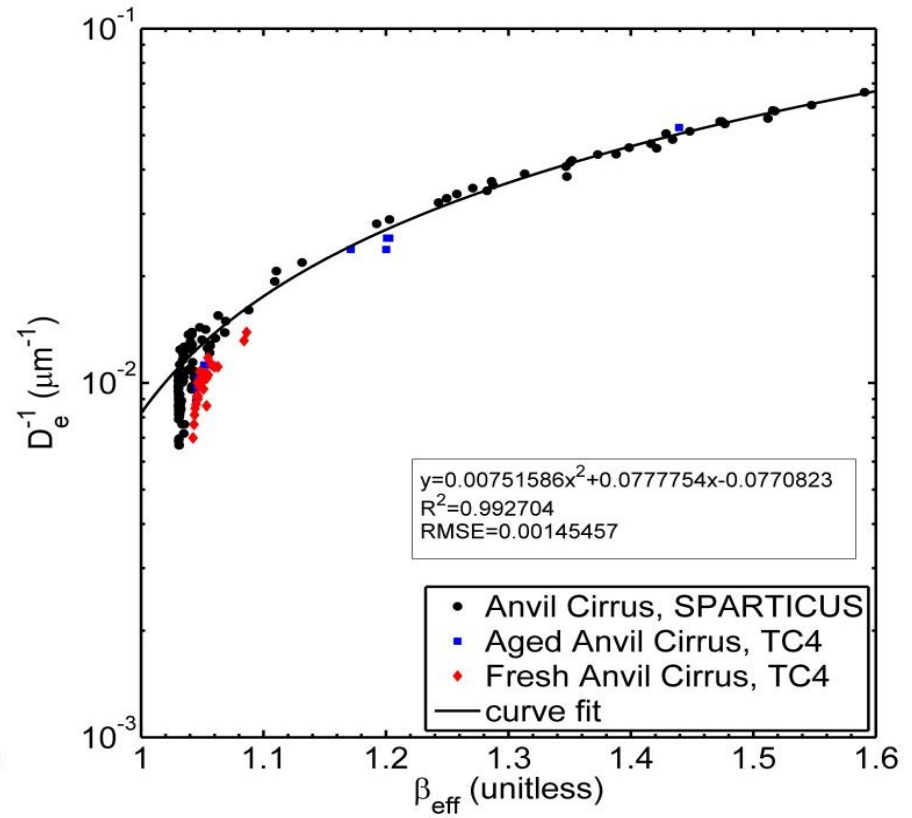
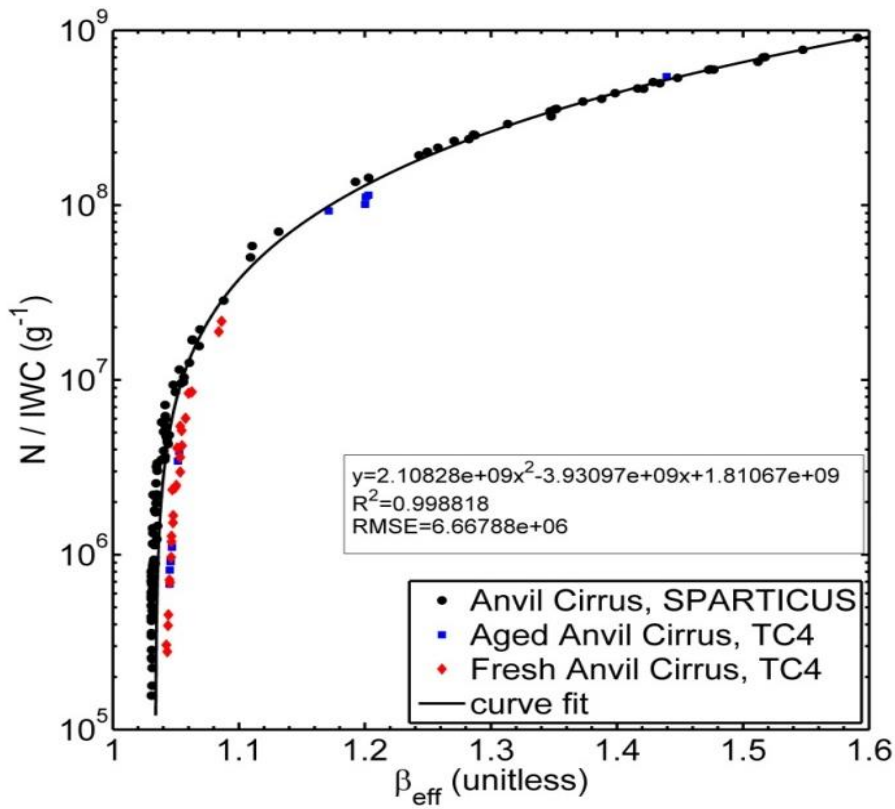
In practice, use the ratio of absorption optical depth:

$$\beta = \tau(12 \mu\text{m}) / \tau(10.6 \mu\text{m}) = \bar{Q}_{\text{abs}}(12 \mu\text{m}) / \bar{Q}_{\text{abs}}(10.6 \mu\text{m}).$$

An effective β that includes scattering effects, β_{eff} , is a standard retrieval product from the imaging infrared radiometer aboard the CALIPSO satellite.

The Retrieval Equation

$$N = \frac{\rho_i [2 / \bar{Q}_{abs}(12 \mu m)] \tau_{abs}(12 \mu m) D_e}{3 \Delta z_{eq}} \left(\frac{N}{IWC} \right)$$



$$N = \frac{\rho_i [2/ \bar{Q}_{abs}(12 \mu m)] \tau_{abs}(12 \mu m) D_e}{3 \Delta z_{eq}} \left(\frac{N}{IWC} \right)$$

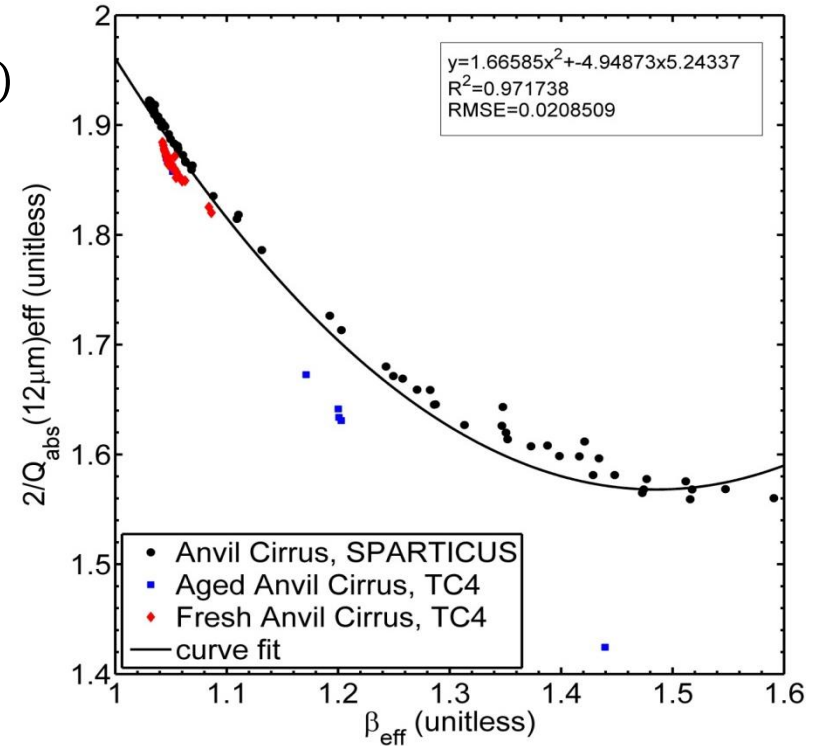
Visible optical depth = $[2/ \bar{Q}_{abs}(12 \mu m)] \tau_{abs}(12 \mu m)$

$$IWC = \frac{\rho_i [2/ \bar{Q}_{abs}(12 \mu m)] \tau_{abs}(12 \mu m) D_e}{3 \Delta z_{eq}}$$

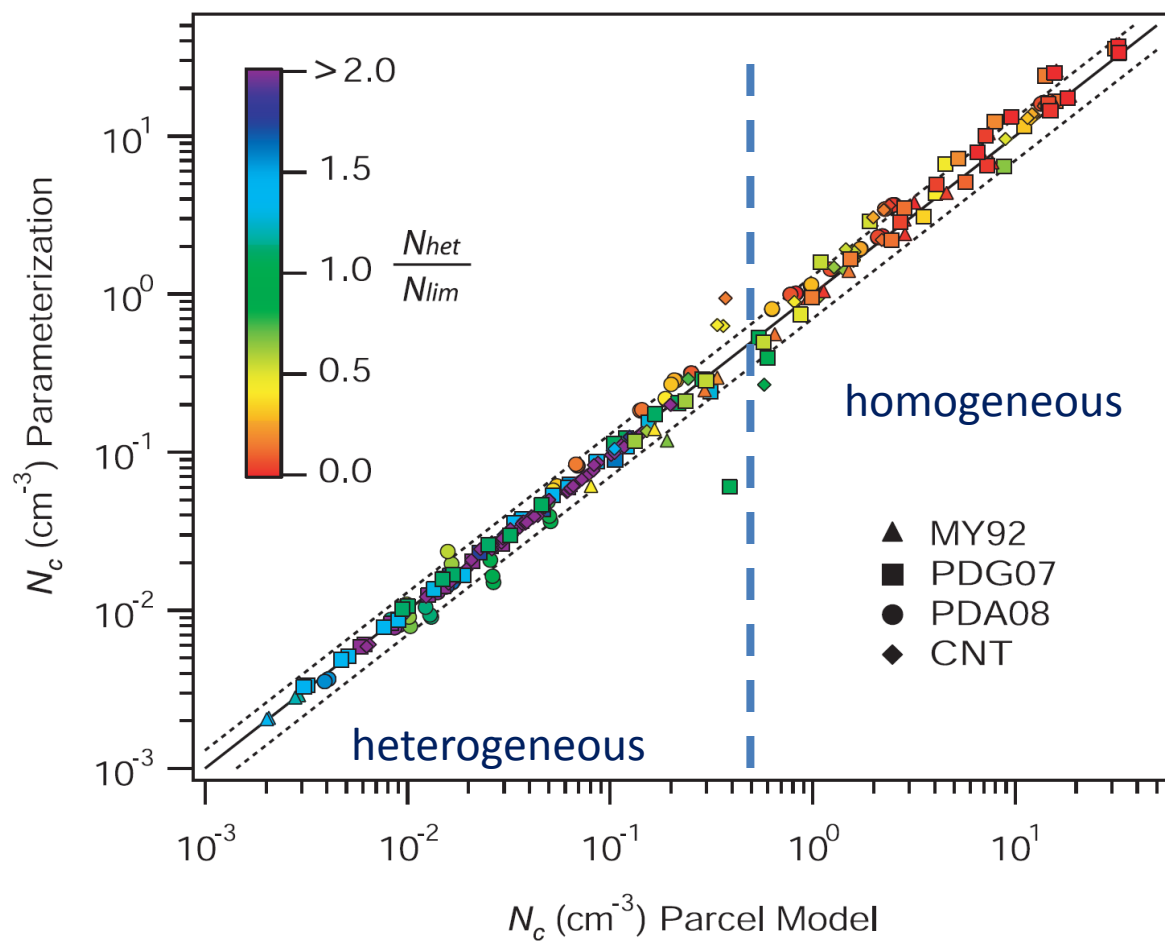
$$IWP = \frac{\rho_i [2/ \bar{Q}_{abs}(12 \mu m)] \tau_{abs}(12 \mu m) D_e}{3}$$

$$extinction\ coeff. = \frac{[2/ \bar{Q}_{abs}(12 \mu m)] \tau_{abs}(12 \mu m)}{\Delta z_{eq}}$$

IWC & extinction refer to mean layer values.



For $\beta_{eff} > 1.485$, $2/ \bar{Q}_{abs} = 1.57$



Cloud formation conditions & aerosol characteristics used to produce this figure from Barahona & Nenes (2009, ACP).

Property	Values
T_o (K)	205–250
V (m s^{-1})	0.04–2
α_d	0.1, 1.0
$\sigma_{g,\text{dry}}$	2.3
N_o (cm^{-3})	200
$D_{g,\text{dry}}$ (nm)	40
N_{dust} (cm^{-3})	0.05–5
N_{soot} (cm^{-3})	0.05–5
θ_{dust}	16°
θ_{soot}	40°
$s_{h,\text{dust}}$	0.2
$s_{h,\text{soot}}$	0.3

Fig. 4. Comparison between N_c from combined homogeneous and heterogeneous freezing predicted by the parameterization and the parcel model for simulation conditions of Table 2 and freezing spectra of Table 1. Dashed lines represent the $\pm 30\%$ difference. Colors indicate the ratio $\frac{N_{\text{het}}}{N_{\text{lim}}}$.

N_{lim} is the limiting IN concentration that completely inhibits homogeneous freezing.

SATELLITE REMOTE SENSING RESULTS

CALIPSO IIR Retrieval Specifications

Resolution is 1km

IIR quality flag= good

IIR pixels co-located with CALIOP track

Types of scene => single-layered clouds not opaque to CALIOP lidar

Cloud base temperature < 235K

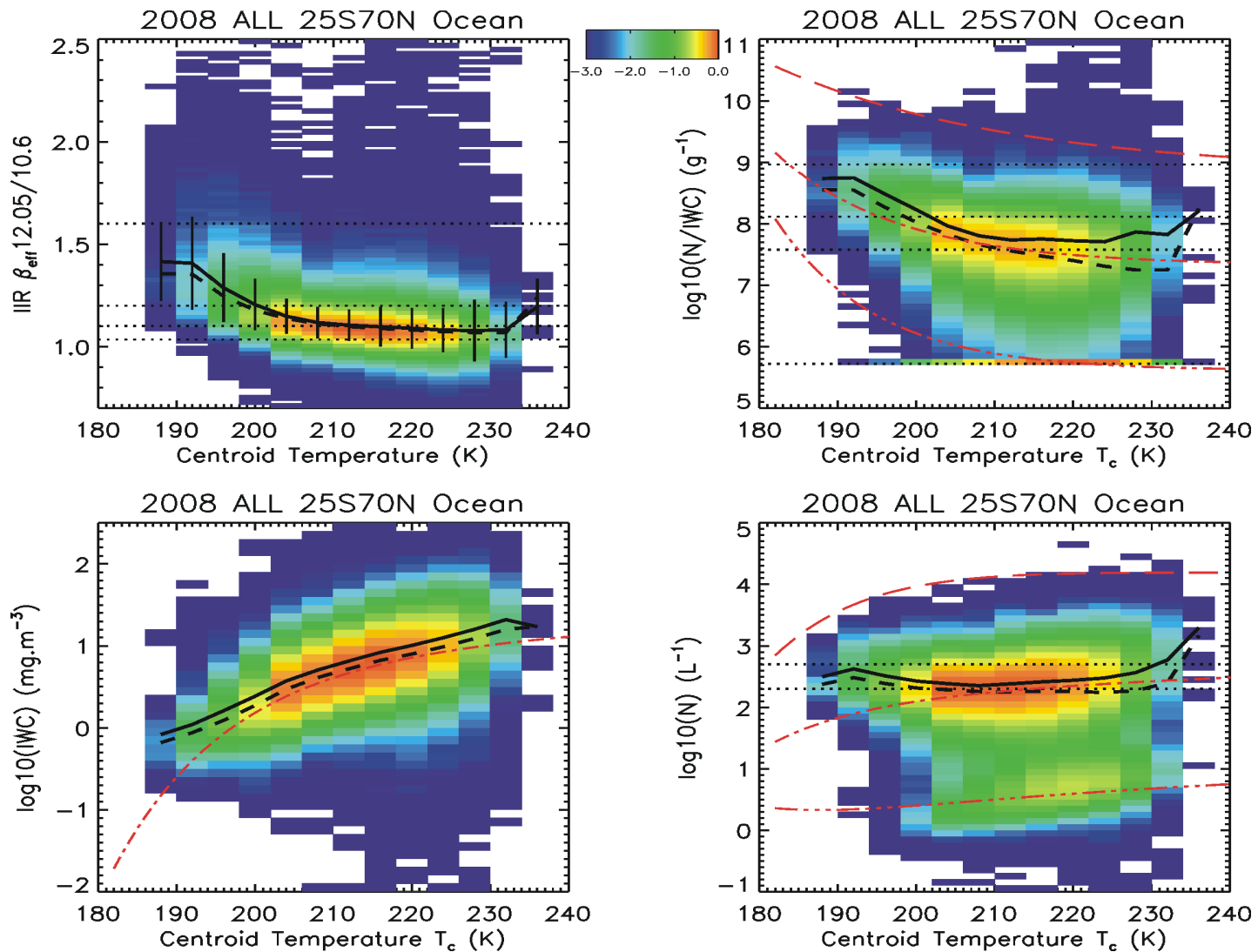
CALIOP Integrated Attenuated Backscatter > 0.01 sr⁻¹

=> $\sim 0.3 < OD_{vis} < \sim 3$

Cloud layer « centroid » temperature = temperature at height dividing the CALIOP attenuated backscatter profile into equal parts.

Reference – Blackbody BTD > 20K

Error estimates (not shown) => measurements ± 0.3 K, reference ± 1 K, blackbody ± 2 K

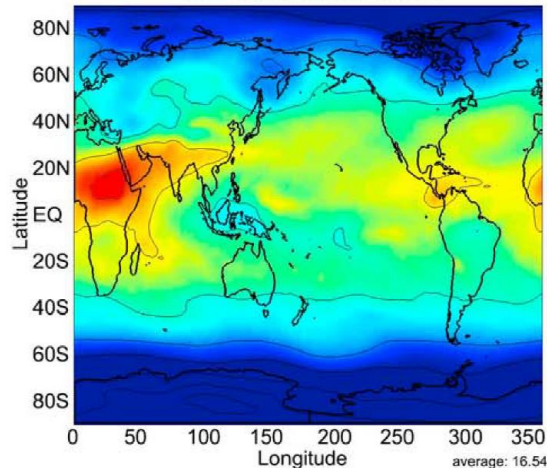


Comparisons of the means (solid curves) and medians (black dashed) of retrieved N/IWC , IWC and N with corresponding in situ measurements from Krämer et al. (2009) shown by the red dashed curves; top and bottom being maximum and minimum values and middle red curve being the middle value. Retrievals are over the ocean for latitudes spanning the range of field campaigns for all seasons. The black dotted horizontal lines in the panel for N correspond to 200 and 500 l^{-1} . Color code: number of samples were normalized to the maximum value (log scale). For $T < 200$ K, sampled cirrus is not TTL cirrus with $OD < 0.3$.

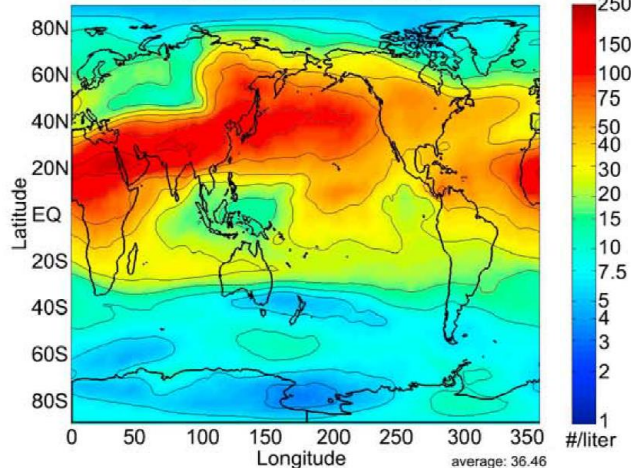
MAM

JJA

Mineral Dust at 200hPa



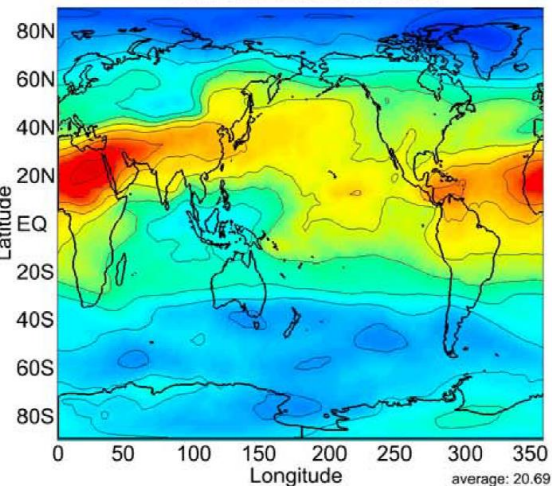
Mineral Dust at 200hPa



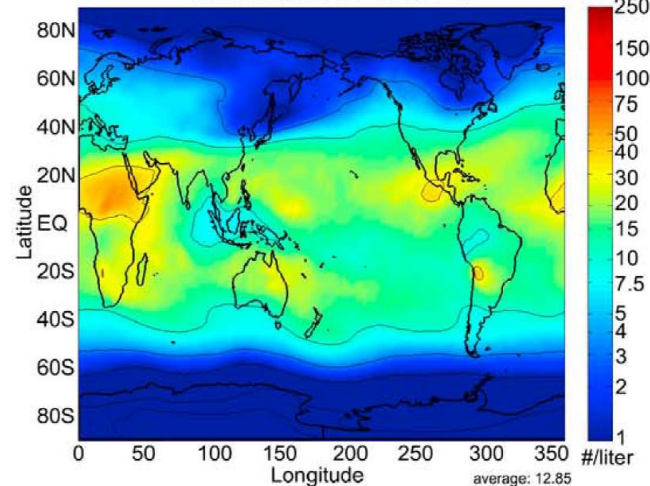
SON

DJF

Mineral Dust at 200hPa



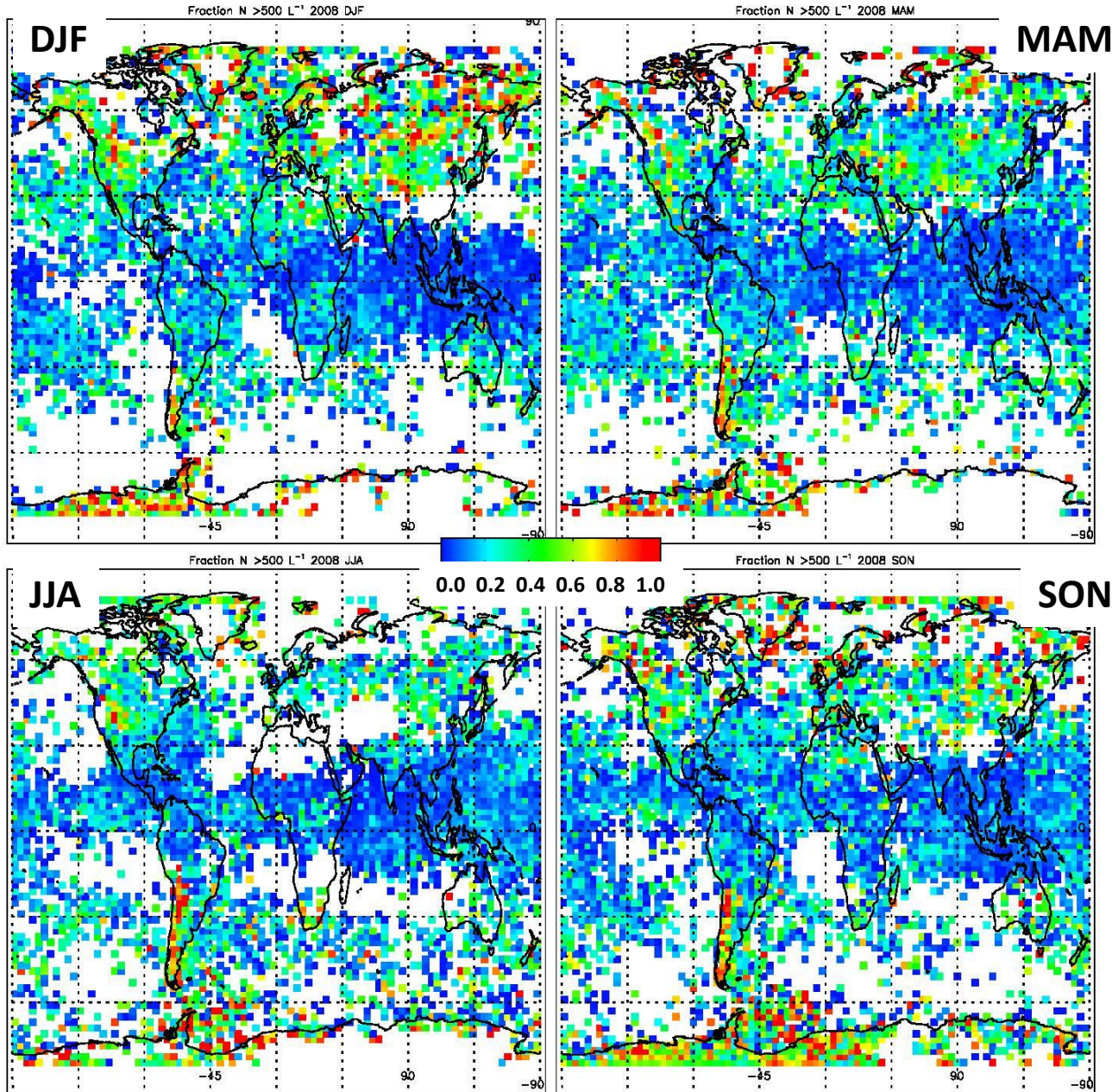
Mineral Dust at 200hPa



CAM5 predictions of mineral dust number concentration at 200 hPa for each season, averaged over 4 years.

From Storelvmo & Herger, 2014, JGR.

The Seasonal Cycle of Hom and Het Cirrus

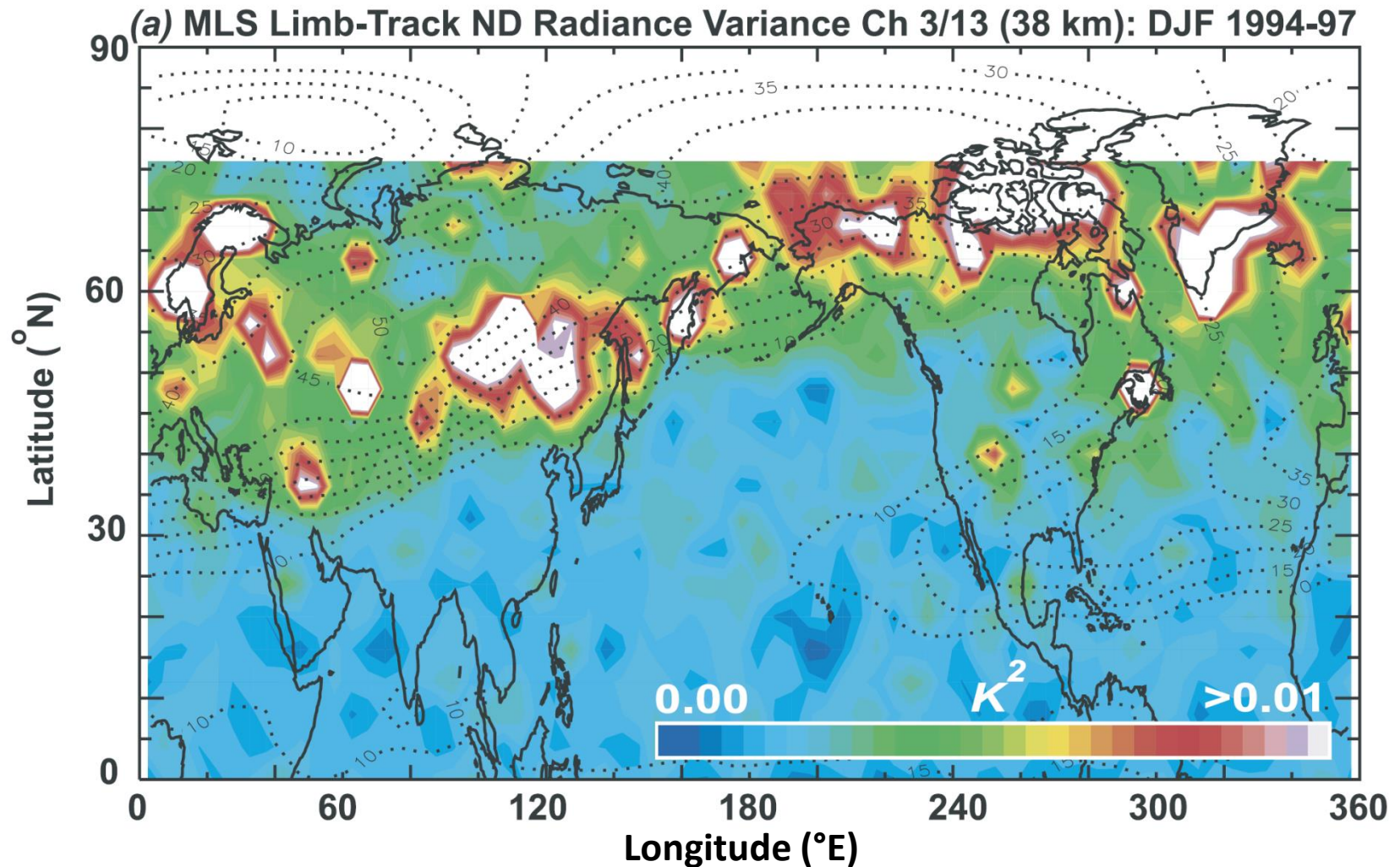


Results for 2008: Fraction of cirrus clouds having $N > 500 \text{ liter}^{-1}$. Such cirrus are most likely formed by homogeneous ice nucleation (hom), and the fraction of these cirrus are shown for each season.

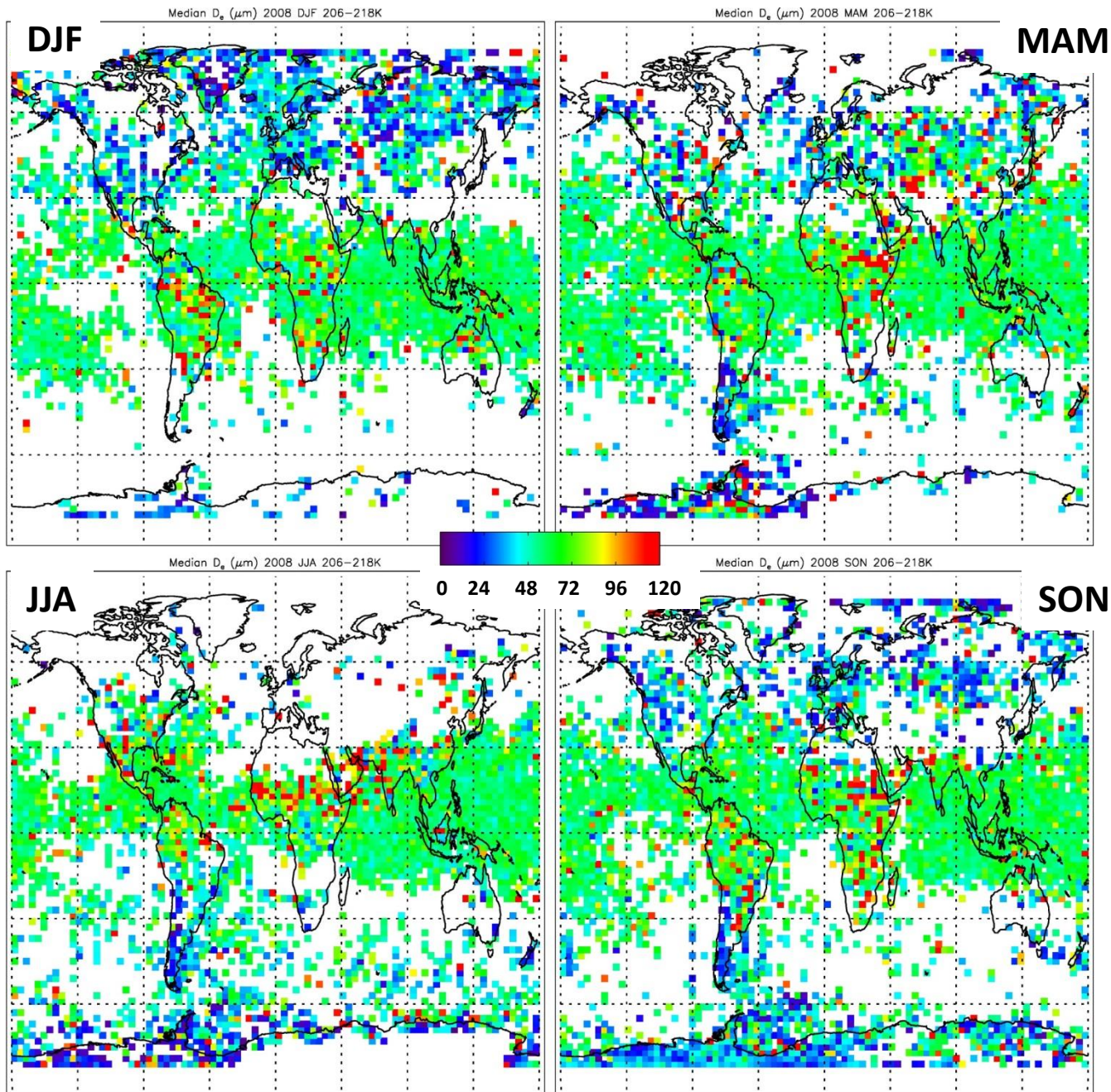
Legend: winter, spring, summer & fall => DJF, MAM, JJA, & SON.

Results are consistent with Cziczo et al. (2013, Science), and have been validated wrt TC4 and ATTREX.

Correspondence of winter hom cirrus with wave cloud intensity



Variations from MLS channels 3/13 limb-track measurements ($z \sim 38$ km) during north-descending orbit segments in the N. Hemisphere winter stratosphere. Dotted contour lines are UKMO mean stratospheric winds between ~ 6.8 & 4.6 hPa. From Jiang et al., JGR, 2004.



Median effective diameter D_e for cirrus clouds residing in the temperature range of 206-218 K. The color bar shows the D_e value in μm . Each panel shows one season as defined by the months DJF, MAM, JJA & SON. Relatively few cirrus exist at these temperatures north of 30°N during summer, although more exist (but still relatively few) at warmer temperatures.

Working Hypothesis

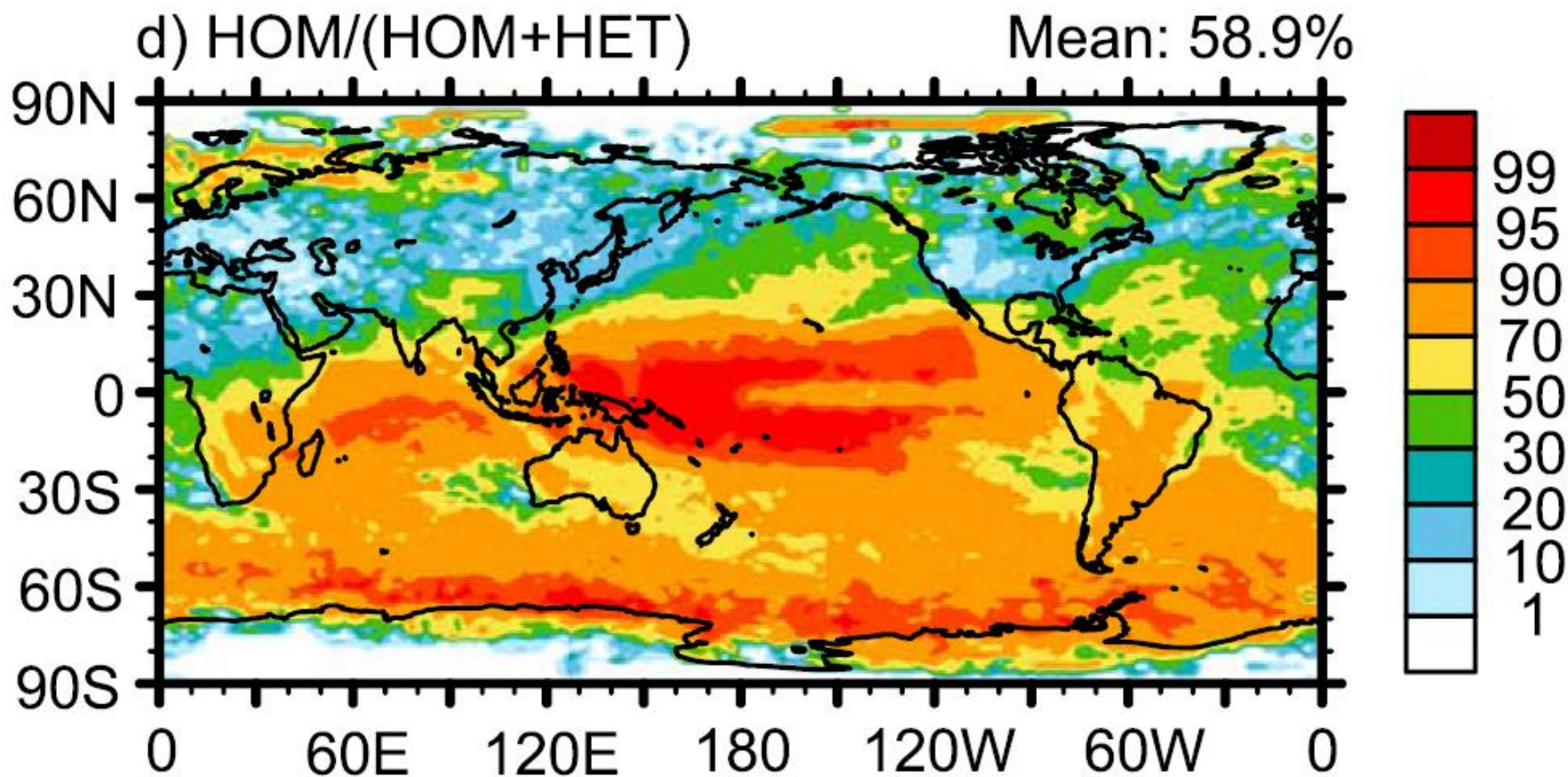
These retrievals show a pronounced cirrus seasonal cycle in the N. Hemisphere over land north of 30°N latitude in terms of both cloud amount and microphysics, with greater cloud cover, higher N and smaller D_e during the winter season. We postulate that this is partially due to the seasonal cycle of deep convection that replenishes the supply of ice nuclei (IN) at cirrus levels, with homogeneous ice nucleation (henceforth hom) prevailing during boreal winter north of 30°N where deep convection is rare and snow often covers the ground, resulting in lower IN and higher N concentrations. In addition, hom cirrus tend to occur over mountainous terrain, possibly due to stronger, more sustained updrafts in orographic waves.

Over oceans, heterogeneous ice nucleation appears to prevail based on the lower N and higher D_e observed. Due to the relatively smooth ocean surface, lower amplitude atmospheric waves at cirrus cloud levels are expected.

Over pristine Antarctica, IN concentrations are expected to be minimal, allowing hom to dominate. Accordingly, over Antarctica cirrus clouds exhibit relatively high N and small D_e throughout the year.

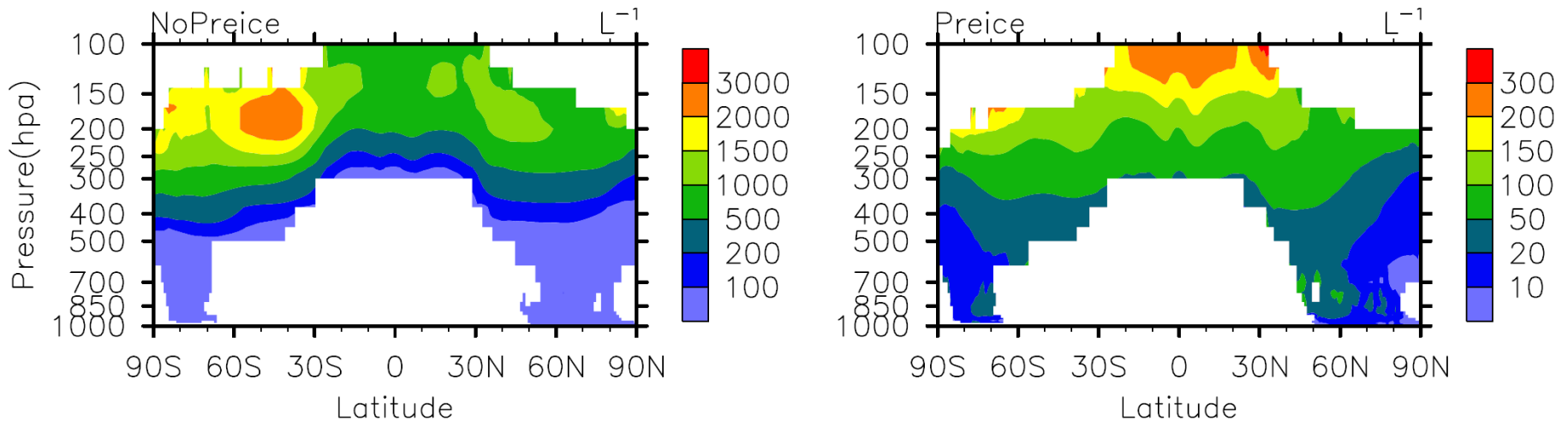
CAM5 simulation with pre-existing ice and 0.1% of 2ndary organic aerosols acting as IN; from Penner et al., 2015, GRL. Hom dominates in TWP with het dominating in N. Hemisphere, mid- & high latitudes.

PRE+SOAIN01



Treatment of ice nucleation in CAM5.3, without and with pre-existing ice

From Shi et al., 2015, ACP



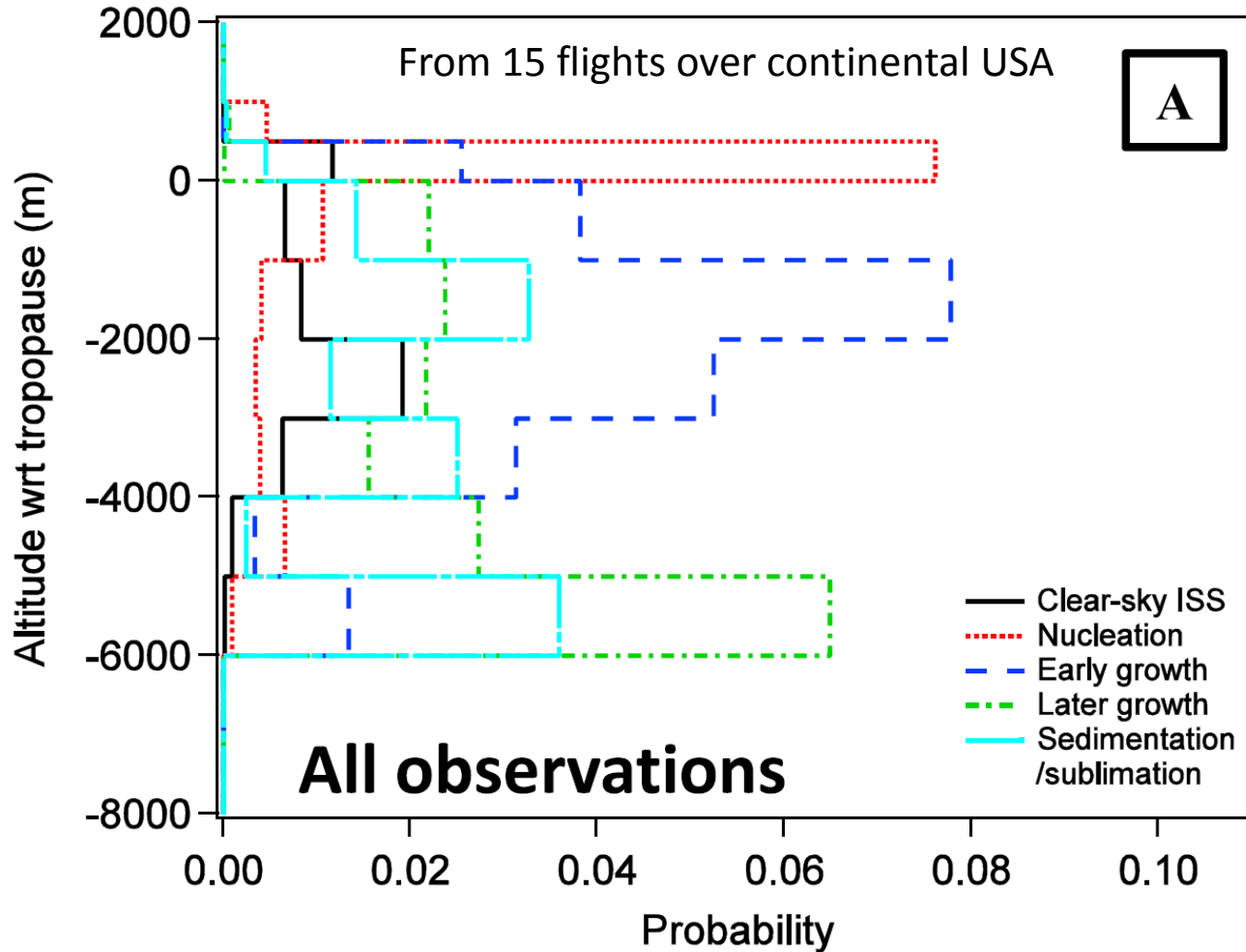
Annual zonal mean for in-cloud ice particle number concentration, N_i , from NoPreice (left) and Preice (right) experiments. Note the different color bars.

Pre-ice reduces the occurrence of hom, especially in the mid- and high-latitudes by a factor of ~ 10 . This trend is opposite to the N_i trend from the CALIPSO retrievals over land.

QUESTION: DOES ICE NUCLEATION IN CIRRUS CLOUDS ALWAYS OCCUR IN THE PRESENCE OF PRE-EXISTING ICE?

How good is the pre-existing ice assumption in the nucleation zone near cloud top?

From Diao et al., 2015, JGR



Ice from a previous time-step has grown for 30 minutes; thus the ice surface area is considerable. But in situ cirrus ice tends to be nucleated near cloud top and then falls to lower levels. The nucleation zone near cloud top may contain residual small crystals but ice surface area should be minimal.

Summary and Conclusions

A new understanding of absorption differences in satellite split-window channels has resulted in a new retrieval method for semi-transparent cirrus clouds ($0.3 < OD < 3.0$). Using the Imaging Infrared Radiometer (IIR) aboard CALIPSO, ice particle number concentration N , D_e , IWC, IWP and visible optical depth (OD) are retrieved for single-layer cirrus having cloud base temperature $T < 235$ K. The retrieval is sensitive to small crystals due to the absorption type.

A cirrus cloud seasonal cycle is evident over land in the N. Hemisphere, with hom cirrus common during winter north of 30° latitude, especially over mountainous terrain. Het cirrus dominate the tropics and oceans and are more common during summer over land at mid-latitudes. Hom cirrus prevail during all seasons over Antarctica.

Recent CAM5 simulations are strongly affected by pre-existing ice and show hom and het prevailing in approximately opposite ways relative to the CALIPSO results. Ice nucleation conditions inferred from measurements appear inconsistent with conditions implied by the pre-existing ice assumption. Should we assume pre-existing ice for all cirrus clouds?

Extra Slides

For Lagrangian evolution of in situ cirrus, the ice nucleation phase is relatively brief; much less than a CAM5 30-minute time-step.

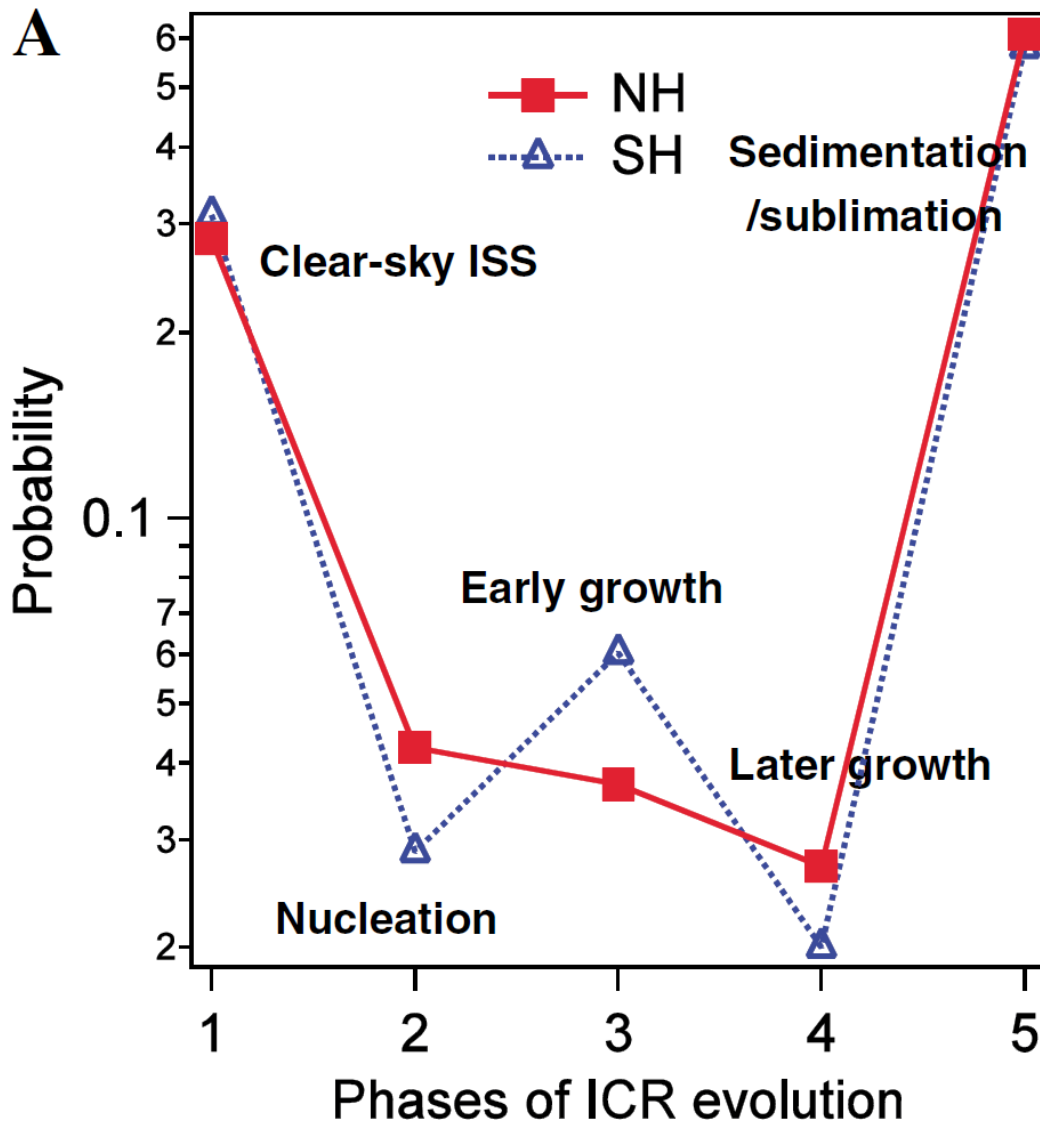
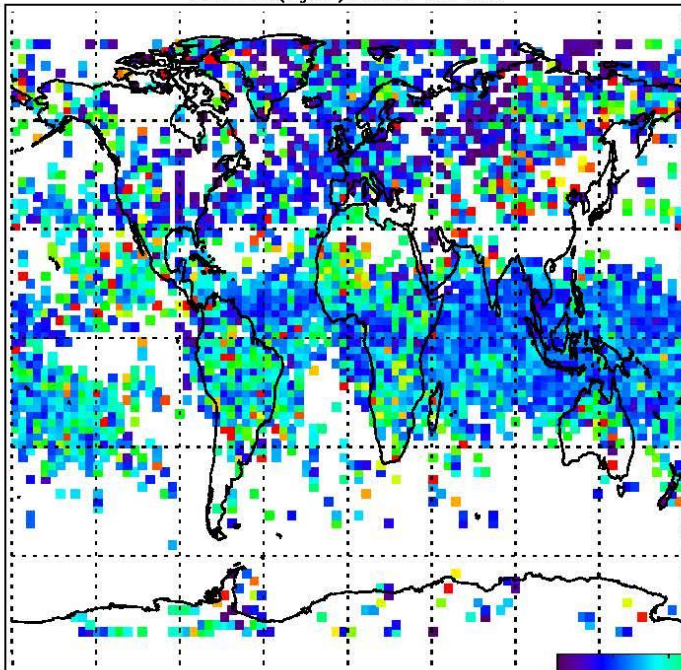


Figure from Diao et al.,
2014, GRL.

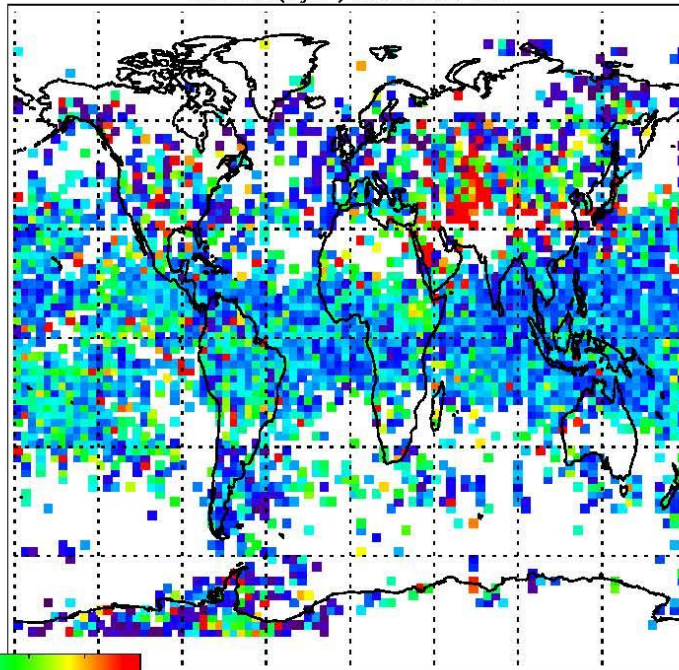
ICR = ice crystal region
ISSR = ice supersaturation
region

Phase 1: ISSR alone
Phase 2: ICRs inside ISSRs
Phase 3: ICRs & ISSRs intersect
Phase 4: ISSRs inside ICRs
Phase 5: ICRs without ISSRs

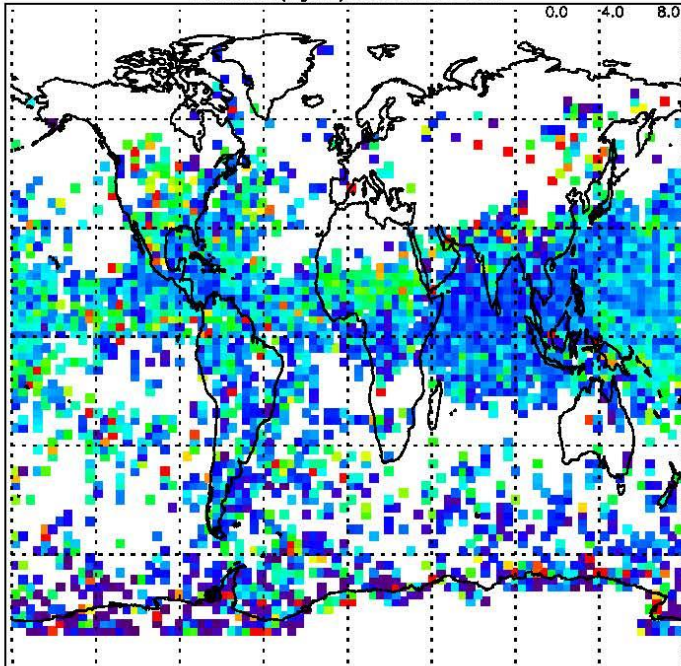
Median IWC ($\text{mg}\cdot\text{m}^{-3}$) 2008 DJF 206–218K



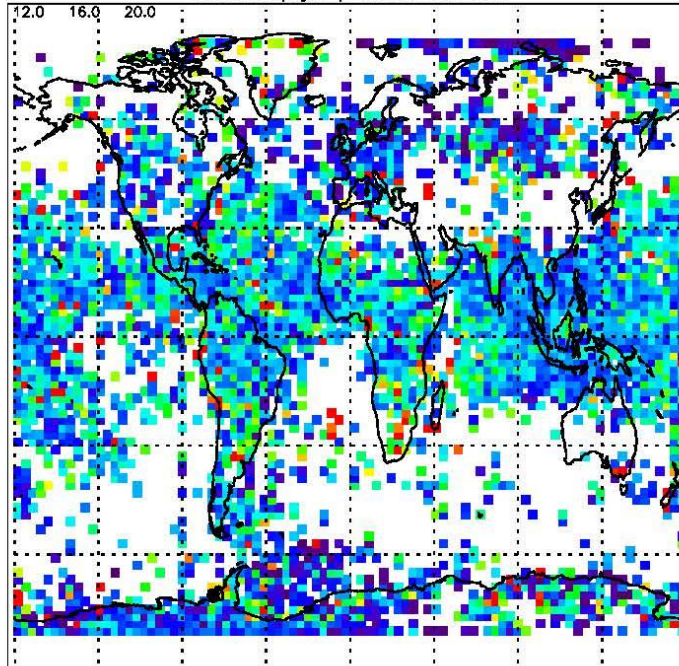
Median IWC ($\text{mg}\cdot\text{m}^{-3}$) 2008 MAM 206–218K



Median IWC ($\text{mg}\cdot\text{m}^{-3}$) 2008 JJA 206–218K



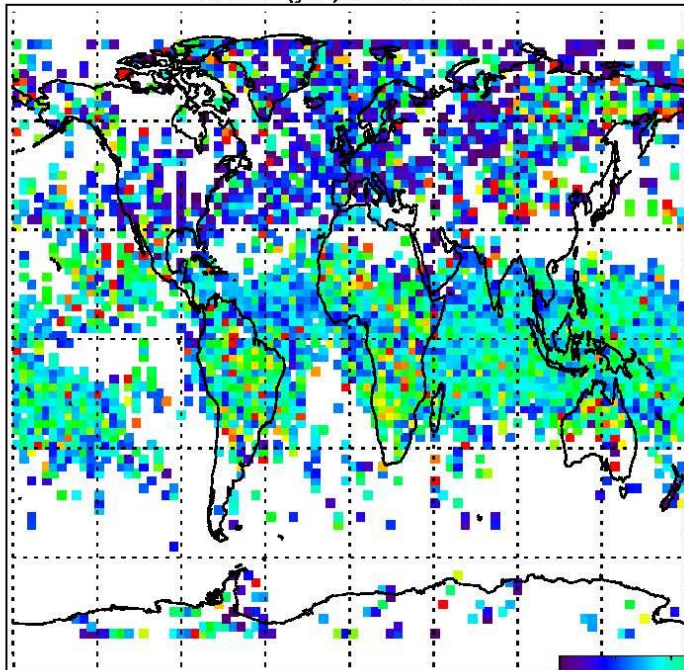
Median IWC ($\text{mg}\cdot\text{m}^{-3}$) 2008 SON 206–218K



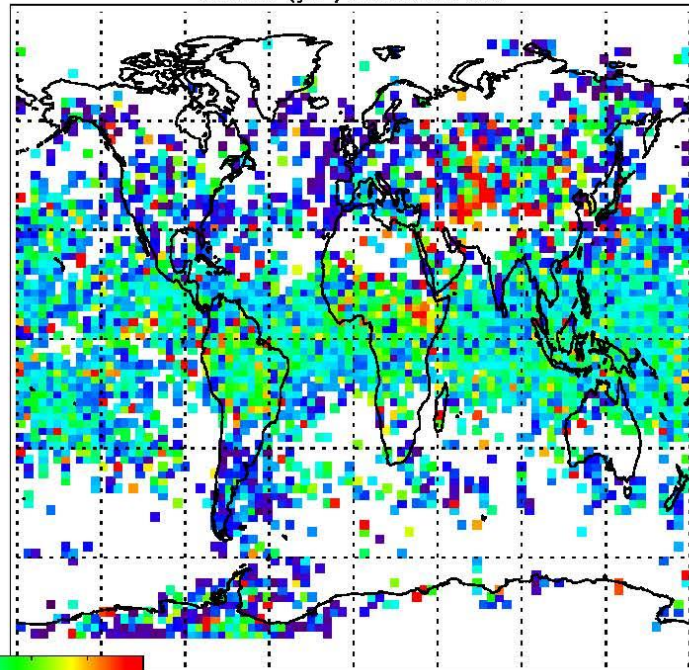
0.0 4.0 8.0

12.0 16.0 20.0

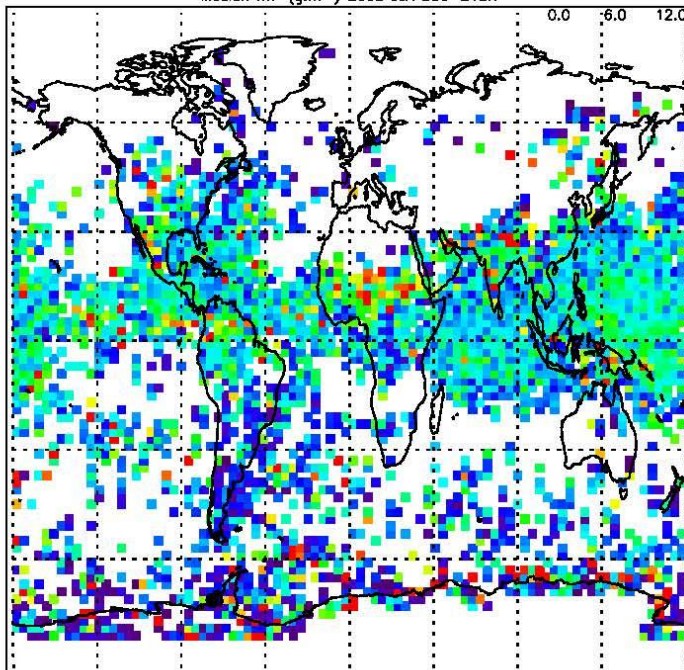
Median IWP ($\text{g}\cdot\text{m}^{-2}$) 2008 DJF 206–218K



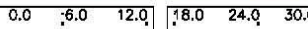
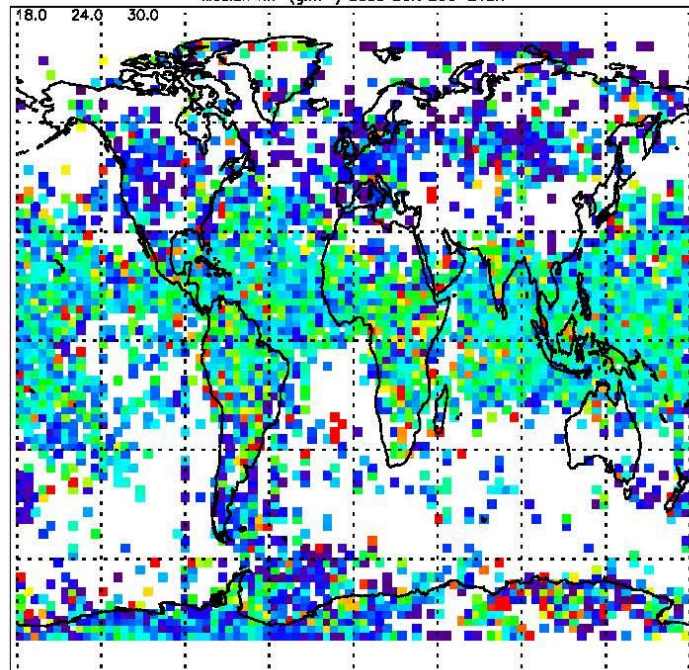
Median IWP ($\text{g}\cdot\text{m}^{-2}$) 2008 MAM 206–218K



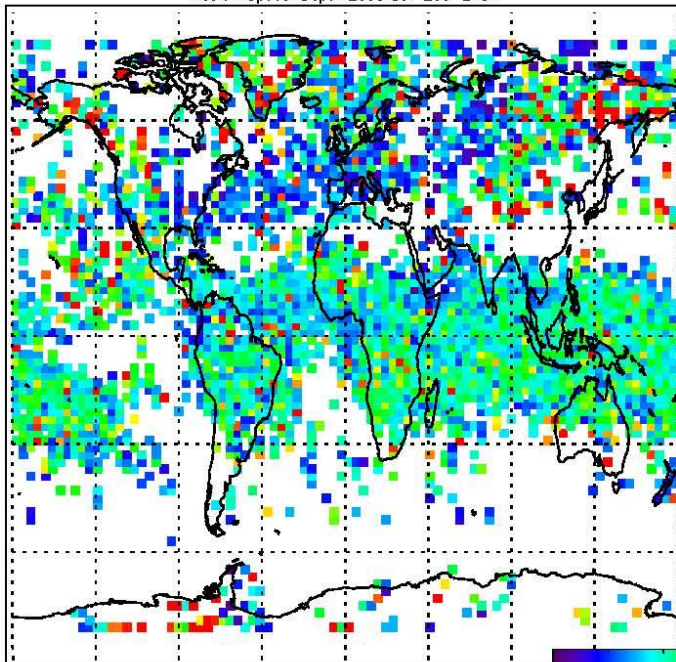
Median IWP ($\text{g}\cdot\text{m}^{-2}$) 2008 JJA 206–218K



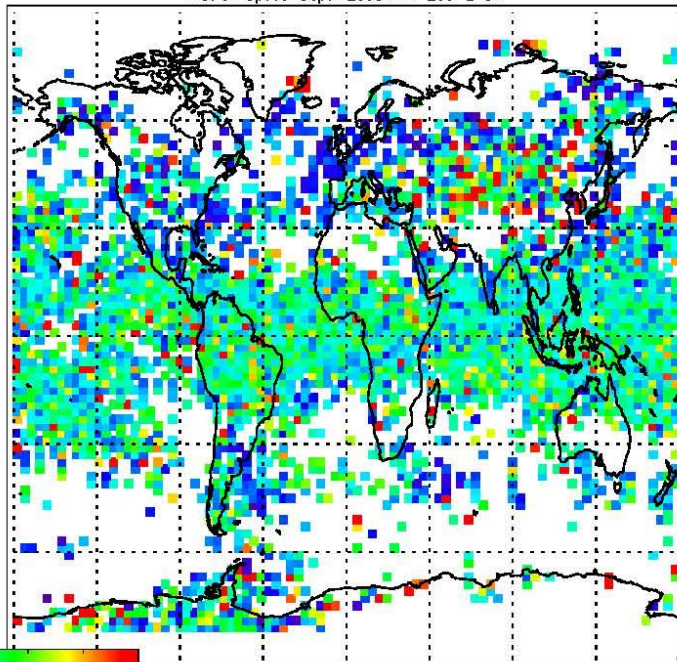
Median IWP ($\text{g}\cdot\text{m}^{-2}$) 2008 SON 206–218K



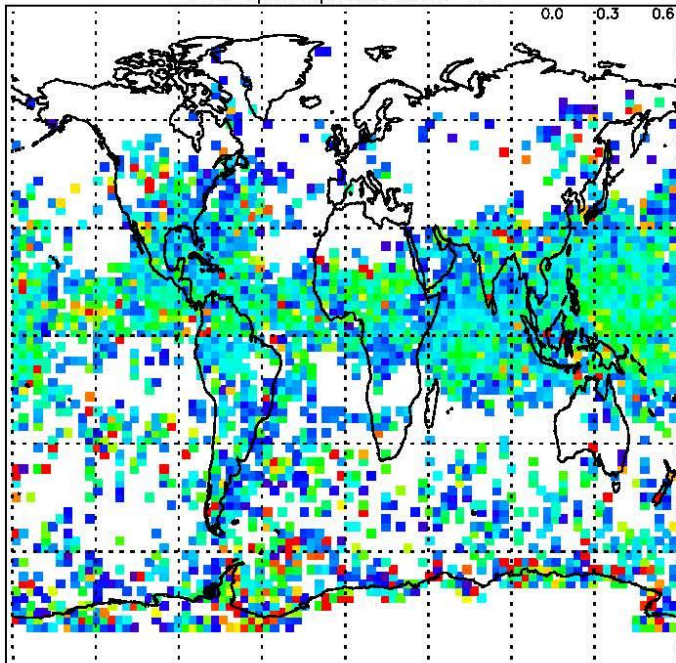
Median Optical Depth 2008 DJF 206–218K



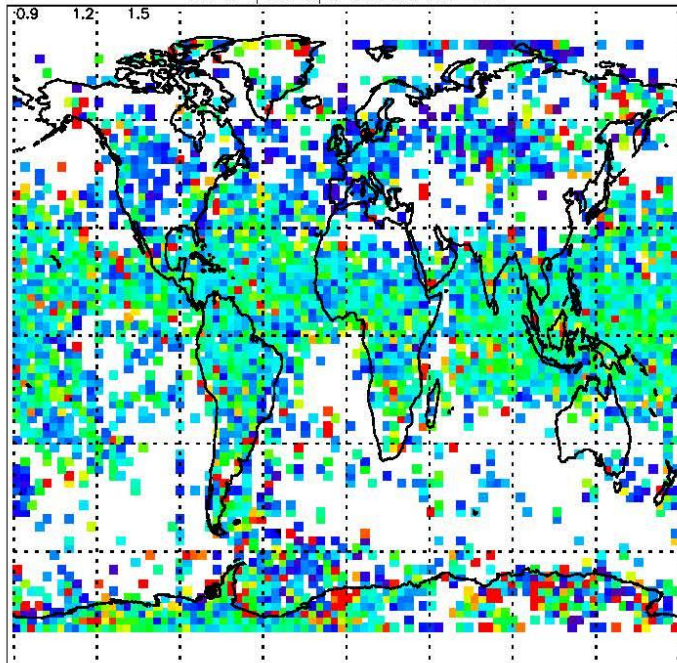
Median Optical Depth 2008 MAM 206–218K



Median Optical Depth 2008 JJA 206–218K



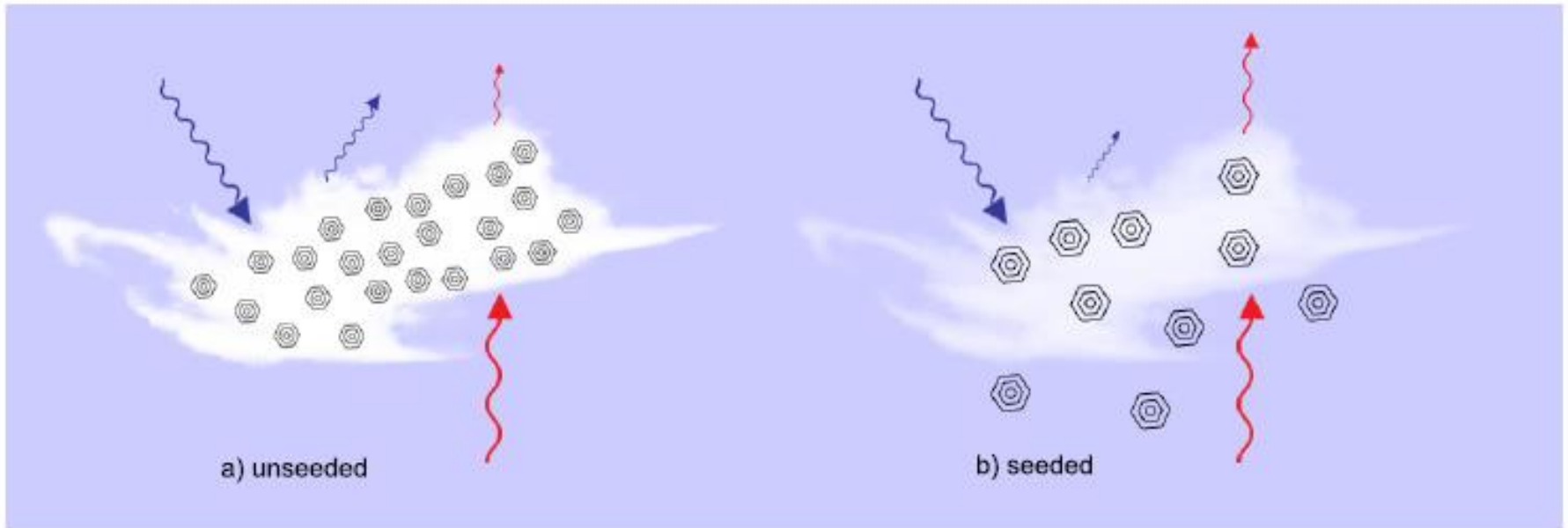
Median Optical Depth 2008 SON 206–218K



0.0 0.3 0.6

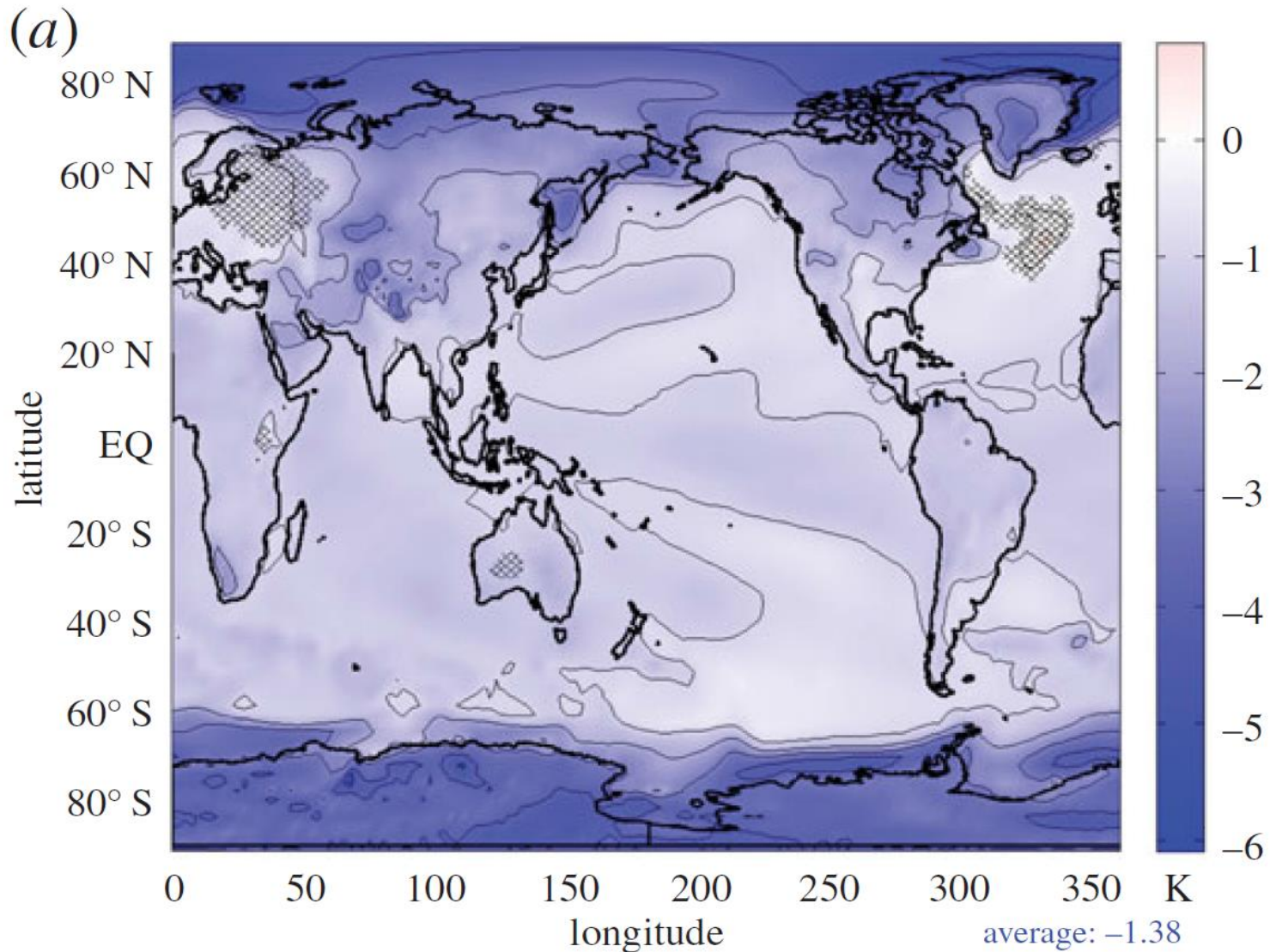
0.9 1.2 1.5

Conceptual diagram of cirrus cloud thinning, taken from Storelvmo et al. 2013, GRL.



Efficient ice nuclei are introduced into an upper troposphere depleted of these ice nuclei so that instead of forming cirrus clouds by homogeneous ice nucleation (hom), cirrus are formed by heterogeneous ice nucleation (het). Het cirrus have larger ice crystals that fall faster, thinning the cirrus to allow more thermal radiation to escape to space, cooling the planet.

Surface Cooling from Cirrus Climate Engineering: From Storelvmo et al. 2014



Surface air temperature (K) response to seeding. Hatching indicates regions where the difference between SEEDING and CONTROL is not statistically significant.

Relating CALIPSO β_{eff} retrievals to in situ measurements of β_{eff}

RETRIEVAL PROTOCOL:

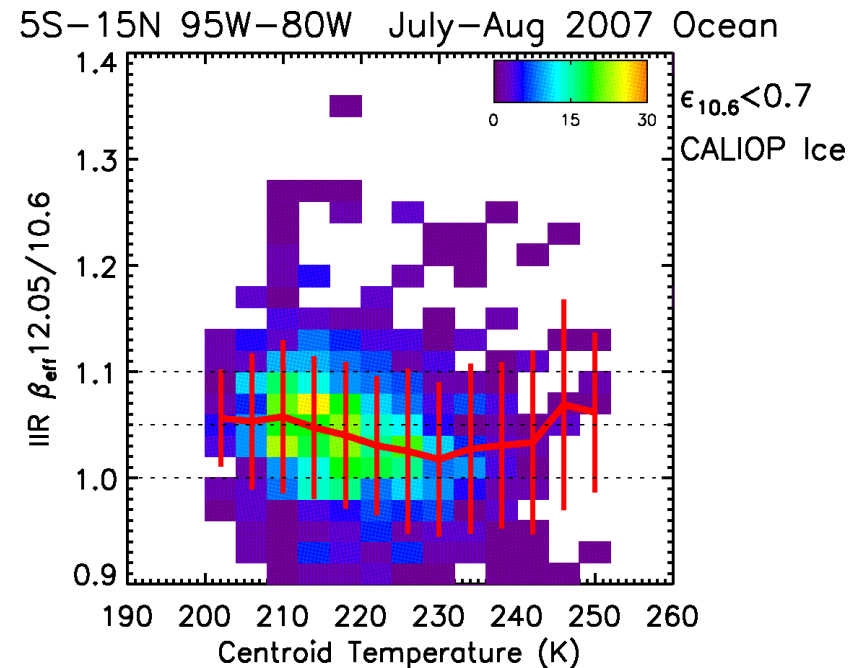
Single-layered clouds, IIR pixels co-located with CALIOP lidar track

CALIOP lidar: cloud layers classified as ice by CALIOP, randomly oriented ice and horizontally oriented ice, high and medium confidence.

Color code: number of samples

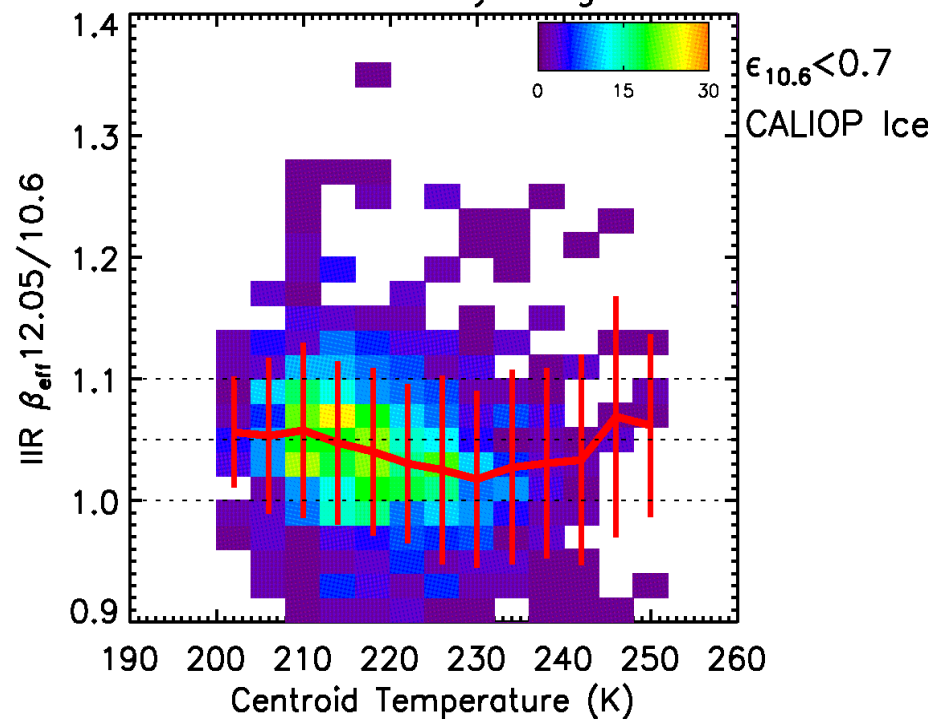
In red: mean values and standard deviations

Cloud centroid temperature: temperature at the centroid altitude of the CALIOP attenuated backscatter profile.



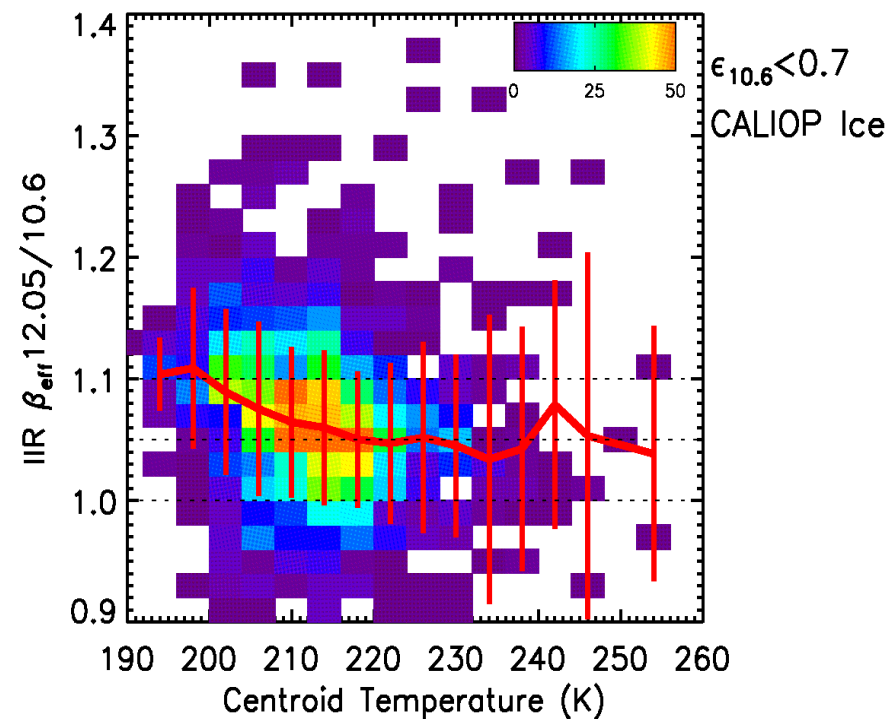
TC4 2007

5S-15N 95W-80W July-Aug 2007 Ocean



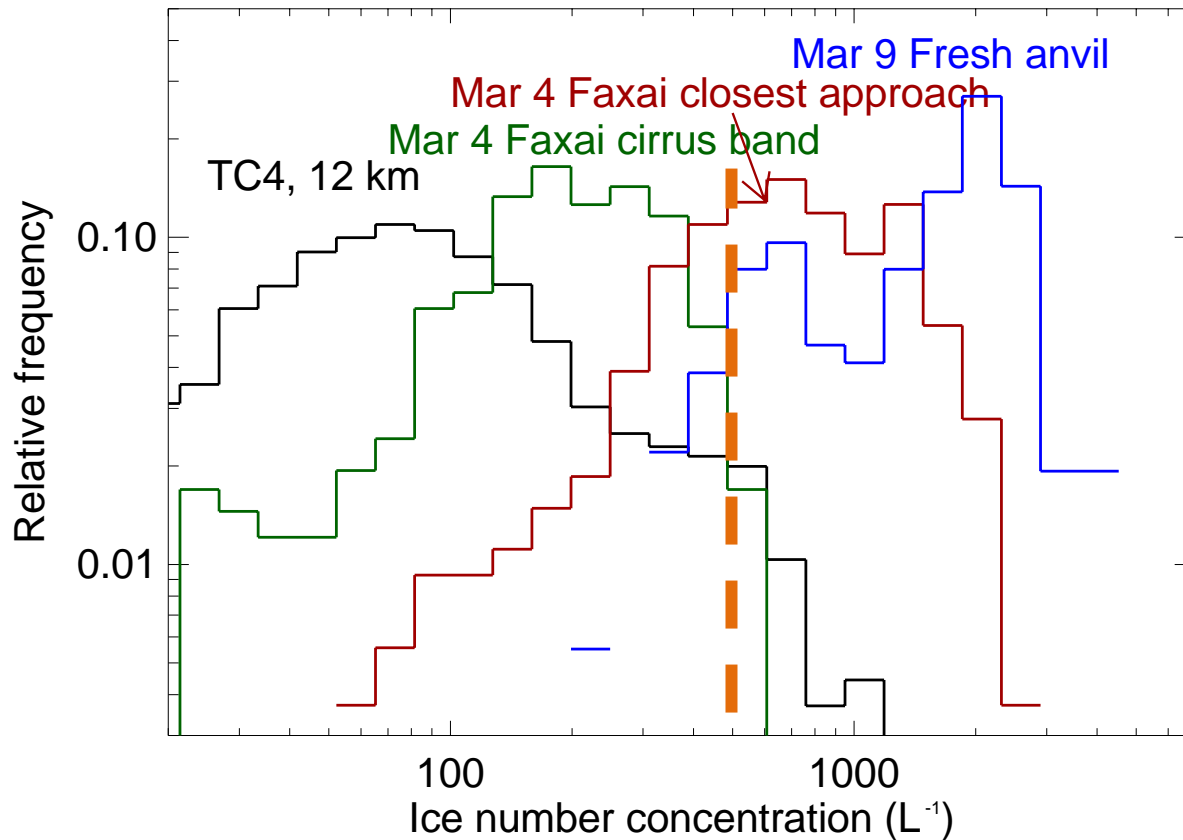
ATTREX 2014

0N-20N 130E-160E Feb10-March14 2014 Ocean



Slide courtesy of E. Jensen, P. Lawson, S. Woods, S. Lance, B. Gandrud;
NASA ATTREX Science Team Meeting

2DS ice concentrations



- ATTREX anvils (14–16 km) generally have larger ice concentrations than lower TC4 anvils (<12 km) [1]
- Differences between ATTREX cases likely attributable to location in cloud, cloud age, etc.

[1] Differences between TC4 2DS and ATTREX 2DS (Hawkeye) cannot be ruled out